A structure-based mechanism of cisplatin resistance mediated by glutathione transferase P1-1

Anastasia De Luca[a,1], Lorien J. Parker[b,c,1], Wee Han Ang[d], Carlo Rodolfo[a], Valentina Gabbarini[a], Nancy C. Hancock[b], Francesca Palone[a,e], Anna P. Mazzetti[a], Laure Menin[f], Craig J. Morton[b,c], Michael W. Parker[b,c,2,3], Mario Lo Bello[a,2], and Paul J. Dyson[f,2,3]

[a]Department of Biology, University of Rome Tor Vergata, 00133 Rome, Italy; [b]Australian Cancer Research Foundation Rational Drug Discovery Centre, St. Vincent's Institute of Medical Research, Fitzroy, VIC 3065, Australia; [c]Department of Biochemistry and Molecular Biology, Bio21 Molecular Science and Biotechnology Institute, The University of Melbourne, Parkville, VIC 3010, Australia; [d]Department of Chemistry, National University of Singapore, 117506 Singapore; [e]Pediatric Gastroenterology and Liver Unit, Department of Pediatrics, Sapienza University of Rome, 00161 Rome, Italy; and [f]Institut des Sciences et Ingénierie Chimiques, École Polytechnique Fédérale de Lausanne (EPFL), CH-1015 Lausanne, Switzerland

Edited by Robert Huber, Max Planck Institute of Biochemistry, Planegg-Martinsried, Germany, and approved May 23, 2019 (received for review February 28, 2019)

Cisplatin [*cis*-diamminedichloroplatinum(II) (*cis*-DDP)] is one of the most successful anticancer agents effective against a wide range of solid tumors. However, its use is restricted by side effects and/or by intrinsic or acquired drug resistance. Here, we probed the role of glutathione transferase (GST) P1-1, an antiapoptotic protein often overexpressed in drug-resistant tumors, as a *cis*-DDP–binding protein. Our results show that *cis*-DDP is not a substrate for the glutathione (GSH) transferase activity of GST P1-1. Instead, GST P1-1 sequesters and inactivates cisplatin with the aid of 2 solvent-accessible cysteines, resulting in protein subunits cross-linking, while maintaining its GSH-conjugation activity. Furthermore, it is well known that GST P1-1 binding to the c-Jun N-terminal kinase (JNK) inhibits JNK phosphorylation, which is required for downstream apoptosis signaling. Thus, in turn, GST P1-1 overexpression and Pt-induced subunit cross-linking could modulate JNK apoptotic signaling, further confirming the role of GST P1-1 as an antiapoptotic protein.

cisplatin | drug resistance | glutathione transferase | protein crystallography | protein–ligand interactions

Cisplatin [*cis*-diamminedichloroplatinum(II) (*cis*-DDP)] is one of the most successful anticancer agents employed today and is effective against a wide range of solid tumors (1–3), including neuroblastoma (4), the extracranial neoplasm most commonly diagnosed in childhood (5). It has long been established that the mechanism of *cis*-DDP involves DNA intrastrand cross-link formation (6, 7), altering the molecular conformation of the double helix leading to apoptosis. In this context, the many DNA-binding proteins involved in these cellular processes play a fundamental role in the mechanism of *cis*-DDP and have been the subject of intense study (8), but the mode of tumor targeting and other molecular interactions have taken much longer to elucidate. Of note, only 5 to 10% of intracellular Pt is associated with the DNA fraction since, after *cis*-DDP enters the cell, there is a rapid formation of mono- and diaquo species in which 1 or 2 chloride ions are substituted by water molecules (9). These new species are highly reactive toward a number of nucleophilic compounds, including thiols [e.g., glutathione (GSH)] and thiol-containing proteins. Thus, the majority of the drug is bound to proteins, RNA, and small thiol compounds (10), and comparatively little is known about these interactions and their role in the biological consequences of *cis*-DDP administration. It has been suggested that following aquation, intracellular *cis*-DDP can be complexed with GSH and subsequently exported through an ATP-dependent process (11). Notably, GSH depletion has been shown to sensitize formerly *cis*-DDP–resistant cell lines (12). Furthermore, it has recently been shown that simultaneous administration of GSH and *cis*-DDP induces *cis*-DDP resistance in human lung carcinoma A549 cells (13). Others have suggested that *cis*-DDP–GSH conjugation can be mediated by glutathione transferases [GSTs; Enzyme Commission no. 2.5.1.18], and chemosensitivity has been linked to GST levels, in particular GST P1-1 (14, 15). Additionally, GSTs have been linked to regulating the side effects of *cis*-DDP, including protection against ototoxicity (16) and indirectly in promoting nephrotoxicity (17, 18). Indeed, even small increases in resistance can be clinically important, since administration of higher doses of *cis*-DDP to counteract the problem can lead to severe multiorgan toxicities (19). Furthermore, GST P1-1 knockout mice are much more sensitive to the cytotoxic effects of *cis*-DDP than their wild-type (WT) counterparts (20).

GSTs belong to a superfamily of multifunctional enzymes involved in cellular detoxification of many toxic compounds through GSH conjugation. GSTs are dimeric enzymes with an active site on each subunit composed of a specific GSH-binding site (G site) positioned in proximity to a hydrophobic but otherwise nonspecific compound-binding pocket (H site). GST Pi class enzymes, including GST P1-1, are characterized by 2 solvent-accessible cysteine

Significance

The resurgence of platinum-based chemotherapy in the last few years has renewed interest in the field, including clinical studies of cisplatin in combination with resistance modulators. Indeed, cisplatin is one of the most successful anticancer agents, effective against a wide range of solid tumors. However, its use is restricted by side effects and/or by intrinsic or acquired drug resistance. We propose here a new mechanism of cisplatin resistance mediated by glutathione transferase (GST) P1-1, as a cisplatin-binding protein. Our results show that cisplatin can be inactivated by this protein with the aid of 2 solvent-accessible and reactive cysteines. These findings may constitute the basis for the design and synthesis of new GST inhibitors able to circumvent cisplatin resistance.

Author contributions: A.D.L., L.J.P., M.L.B., and P.J.D. designed research; A.D.L., L.J.P., W.H.A., C.R., V.G., N.C.H., F.P., A.P.M., and L.M. performed research; A.D.L., L.J.P., W.H.A., C.R., L.M., C.J.M., M.W.P., and M.L.B. analyzed data; and A.D.L., L.J.P., C.J.M., M.W.P., M.L.B., and P.J.D. wrote the paper.

The authors declare no conflict of interest.

This article is a PNAS Direct Submission.

Data deposition: The models reported in this paper have been deposited in the Research Collaboratory for Structural Bioinformatics Protein Data Bank, https://www.rcsb.org/ [PDB ID nos. 5DJM (*cis*-DDP complex) and 5DJL (*cis*-DDP–GSH complex)].

[1]A.D.L. and L.J.P. contributed equally to this work.

[2]M.W.P., M.L.B., and P.J.D. contributed equally to this work.

[3]To whom correspondence may be addressed. Email: mparker@svi.edu.au or paul.dyson@epfl.ch.

This article contains supporting information online at www.pnas.org/lookup/suppl/doi:10.1073/pnas.1903297116/-/DCSupplemental.

residues that affect catalytic activity when modified: C47, located near the G site and fundamental for maintaining the conformation and stability of the G site; and C101, located at the dimer interface, which can form a disulfide bond with C47, requiring a large-scale conformational change that leads to inactivation of the enzyme (21, 22). To date, several drugs, such as chlorambucil and ethacrynic acid (23), have been shown to be effective substrates or inhibitors of GSTs, whereas other drugs, such as doxorubicin, do not interact with this family of enzymes (24), although inhibition of GST P1-1 increases sensitivity of certain cancer cell lines to this anticancer compound (25). Human GST P1-1 is overexpressed in several solid tumors and in different tumor cell lines resistant to anticancer drug treatment (26) and has therefore been linked to resistance. Besides the central role of GSTs in cancer and the acquisition of drug resistance, plant GSTs (Phi, Zeta, Tau, and Theta GSTs) are fundamental in herbicide tolerance. Indeed, it has been shown that these plant enzymes detoxify several classes of electrophilic herbicides (i.e., triazines, chloroacetamides, thiocarbamates, and diphenylethers). Interestingly, plants have 25 or more genes coding for GSTs; the proteins share as little as 10% amino acid identity and each is characterized by a different substrate specificity according to the H-site structure (27, 28)

GSTs also possess a noncatalytic ligand-binding role, functioning as intracellular transporters of various nonsubstrate hydrophobic compounds such as bilirubin, steroids, thyroid hormones, bile salts, and drugs, altering the tissue distribution of these molecules (29). This noncatalytic GST site has been referred to as the ligandin-binding site (or L site) and overlaps with the H site (30). GST P1-1 has other functions involving heterodimerization with different proteins. For example, GST P1-1 has been also identified as a key regulator of cell survival signaling through the interaction with c-Jun N-terminal kinase (JNK). Indeed, GST P1-1 is able to sequester JNK, in a catalytic-independent manner, acting as a negative regulator of this stress kinase (31, 32).

Thus, different regulatory functions of GST P1-1 may play a central role in GST P1-1–mediated resistance to anticancer drugs such as *cis*-DDP. The study presented here investigated the role of GST P1-1 in cellular response to *cis*-DDP using a neuroblastoma cell line (SH-SY5Y) transfected with GST P1-1 and either C47S, C101S, or C47S/C101S mutant enzymes. In neuroblastoma patients, a strong correlation between the level of messenger RNA of *GSTP1-1* and the disease outcome has been demonstrated. Of note, high levels of *GSTP1* were associated with decreased event-free and overall survival (33).

In addition, we evaluate the possibility of enzymatic conjugation between *cis*-DDP and GSH and identify the possible sites of interaction between *cis*-DDP and GST P1-1 with the aid of mass spectroscopy (MS) and protein crystallography.

Results

In Vitro Toxicity of *cis*-DDP Toward Neuroblastoma Cells (SH-SY5Y) Transfected with GST P1-1. A neuroblastoma cell line (SH-SY5Y) was used to investigate the role of GST P1-1 in cellular protection against *cis*-DDP cytotoxicity. The SH-SY5Y cell line was transfected with plasmids coding for WT GST P1-1 and Cys-modified enzymes (C47S, C101S, C47S/C101S). Selected stably transfected clones were analyzed by Western blotting and GST enzymatic activity assays using cell extracts. There was a significant increase in the expression of GST P1-1 in transfected cell lines in comparison with nontransfected cell lines (*SI Appendix*, Fig. S1 *B* and *C*). In parallel, the GST specific activity increased in all transfected clones compared with the controls, in the range of 2- to 5-fold (for the mutants) and 9-fold (for WT) (*SI Appendix*, Fig. S1*C* and Table 1). As this cell line does not possess appreciable amounts of other GST classes (*SI Appendix*, Fig. S1*D* and Table 1), the increases may be attributed specifically to the *GSTP1* transcript.

Cell viability of SH-SY5Y cell lines transfected with WT and mutant *GSTP1* was assessed using the MTS (3-[4,5,dimethylthiazol-2-yl]-5-[3-carboxymethoxy-phenyl]-2-[4-sulfophenyl]-2H-tetrazolium) assay and fluorescence activated cell sorting (FACS) analysis after treatment with graded doses of *cis*-DDP for 24 h (Fig. 1 *A* and *B*) or for 6 h followed by a recovery period for 24 h in a drug-free medium (Fig. 1*C*). Overexpression of WT *GSTP1* significantly protected SH-SY5Y cells from apoptosis induced by *cis*-DDP at all doses tested (Fig. 1*B*). Similar levels of protection were not observed after transfection with the mutated forms of *GSTP1*. Transfection with *GSTP1 C47S* afforded some protection toward cell death, which became more significant at the higher *cis*-DDP doses tested (Fig. 1 *B* and *C*). In contrast, the cells transfected with *GSTP1 C101S* and the double mutation *C47S/C101S* showed no protection to cell death. The same trends were observed in both the 24-h *cis*-DDP incubation and the 6-h incubation followed by a 24-h recovery period, although the degree of cell death was greater with the longer *cis*-DDP incubation (Fig. 1*B*).

***cis*-DDP–GSH Adduct Formation Is Not Affected by GST P1-1.** Adduct formation of *cis*-DDP with GSH was studied in vitro in the absence and presence of GST P1-1 (Fig. 2). During the incubation of *cis*-DDP with GSH in PBS (phosphate buffered saline) at 37 °C, the reaction mixture gradually turned from colorless to yellow. This was accompanied by a spectral change, with the appearance of a broad absorption band at 260 nm, which increased in intensity over the 6-h incubation period (Fig. 2*A*), as previously described (11). The reaction mixtures were purified by anion-exchange chromatography, and the reaction product was further analyzed by electrospray ionization (ESI)-MS.

The enzymatic conjugation of GSH with *cis*-DDP was followed spectrophotometrically at 37 °C in PBS (pH 7.4) or in potassium phosphate buffer (pH 7.0) plus 2 mM NaCl, for 10 min at 260 nm. The data show that the spontaneous reaction rate was not affected by the presence of GST P1-1. At the lower NaCl concentration, the spontaneous rate of conjugation between GSH and *cis*-DDP was greater and increased with the addition of GST P1-1, but only slightly—that is, not proportionately to the enzyme concentration (Fig. 2*C*).

Table 1. Enzymatic activity of GST P1-1 in cells overexpressing GST P1-1 WT and C47S, C101S, and C47S/C101S mutant enzymes

Samples	Specific activity, U/mg	Fold increase vs. SH-SY5Y
SH-SY5Y	0.195 ± 0.09	—
SH-SY5Y pTarget GST P1-1	1.865 ± 0.29	9.6
SH-SY5Y pTarget GST P1-1 C47S	0.476 ± 0.04	2.4
SH-SY5Y pTarget GST P1-1 C101S	0.990 ± 0.07	5.1
SH-SY5Y pTarget GST P1-1 C47S/C101S	0.430 ± 0.06	2.2

The enzymatic activity was determined as reported in the *Materials and Methods* section. The fold increases in the enzymatic activity of the transfected vs. untransfected cells are reported. Values are expressed as means ± SD from 3 independent experiments.

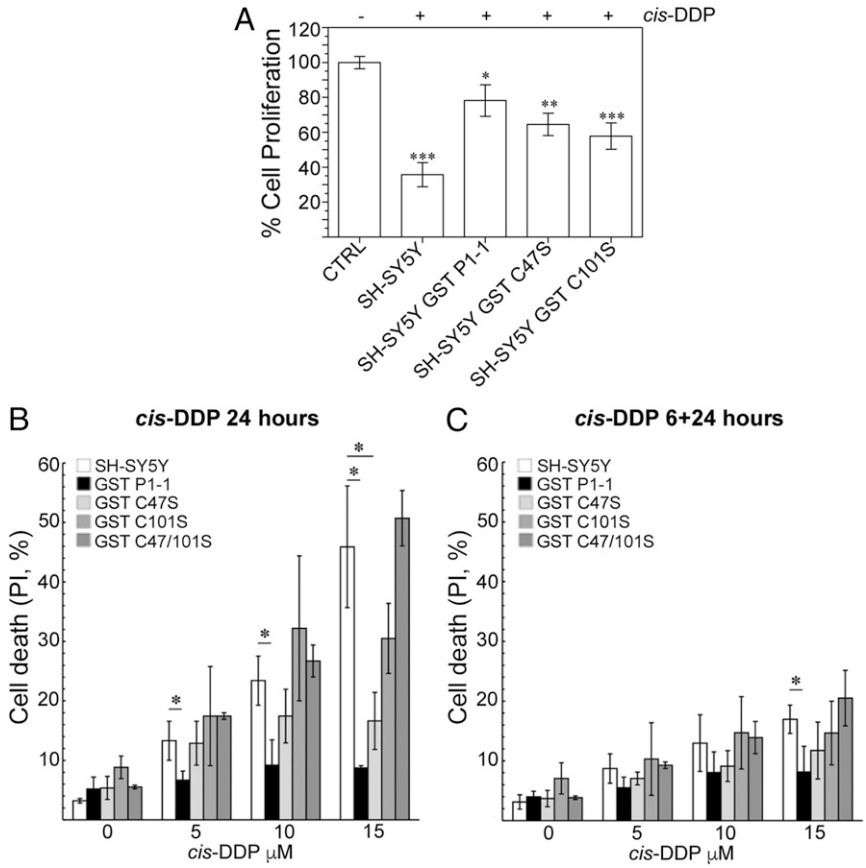

Fig. 1. GST P1-1 protects tumor cells against toxicity and apoptosis following *cis*-DDP treatment. (*A*) Cell viability of SH-SY5Y cell lines expressing WT and mutated GST P1-1, after *cis*-DDP administration. MTS assay was performed on cells treated with 5 μM *cis*-DDP for 24 h. Values, normalized to untreated control cells, are expressed as means ± SD from 3 independent experiments. Statistical significance compared with untreated samples (Student's *t* test): $*P < 0.05$, $**P < 0.01$, $***P < 0.001$. SH-SY5Y, nontransfected cells; −, *cis*-DDP–negative samples; +, after exposure to *cis*-DDP 5 μM for 24 h. (*B*) FACS analysis of apoptosis induction of SH-SY5Y cell lines expressing WT and mutated GST P1-1, after *cis*-DDP administration for 24 h. Values are expressed as means ± SD from 6 independent experiments; $*P < 0.05$. (*C*) Cytofluorometric analysis of apoptosis induction of SH-SY5Y cell lines expressing WT and mutated GST P1-1, after *cis*-DDP administration for 6 h followed by a recovery for additional 24 h. Values are expressed as means ± SD from 6 independent experiments; $*P < 0.05$.

Time Course Inactivation of GST P1-1 with *cis*-DDP. *cis*-DDP was shown to inhibit GST P1-1 activity under certain conditions. When GST P1-1 (10 μM) was incubated without GSH in the presence of 1 mM *cis*-DDP, time-dependent inactivation of the enzyme was observed, which was faster in 10 mM potassium phosphate buffer with 2 mM NaCl than in PBS (pH 7.4) (Fig. 2*D*). After 15 min, the residual activity of GST P1-1 was about 25% of the initial activity. The addition of DTT (DL-dithiothreitol) did not recover the enzymatic activity. In contrast, in the presence of 10 mM GSH in PBS, WT GST P1-1 appeared resistant to *cis*-DDP deactivation (Fig. 2*D*). Inactivation of GST P1-1 occurred more rapidly at low concentrations of NaCl, with the order—in both rate and extent of inactivation—being WT > C47S > C101S. The C101S mutant retained 60% residual activity after 40 min of incubation, whereas the WT was completely inactivated over the same time period (Fig. 2*D*).

***cis*-DDP Treatment Promotes the Cross-Linking of Both GST P1-1 Subunits, in the Absence of GSH, by Platination of C47 and C101.** To assess the platination of GST P1-1 by *cis*-DDP, WT GST P1-1 and its mutants, C47S and C101S, were each incubated in a 1:1 protein-to-drug ratio (50 μM) at 37 °C for up to 72 h. Subsequent analysis by SDS/PAGE (sodium dodecyl sulphate/polyacrylamide gel electrophoresis) under nonreducing conditions showed that the Pt-free WT and C47S samples migrated, for the most part, as a single species with an approximate molecular mass of 24 kDa. ESI-MS analysis confirmed the molecular mass as 23,216 Da in WT GST P1-1 (Fig. 3 *A*, peak A) and 23,199 Da in the C47S mutant (Fig. 3*B*, peak A), corresponding to the anticipated masses of the enzymes calculated from their amino acid sequences. The peaks at 23,346 in the WT (Fig. 3 *A*, peak B) and at 23,330 Da in the C47S mutant (Fig. 3 *B*, peak B) may be attributed to the incomplete removal of the N-terminal methionine residue (labeled with asterisks in Table 2) (34). In contrast, the apo form of the C101S mutant produced 2 bands, at ∼24 and 20 kDa (Fig. 3 *C*, *Inset*). ESI-MS analysis identified a single species with a molecular mass of 23,330 Da (Fig. 3 *C*, peaks A and B), suggesting the bands observed by gel electrophoresis are due to different conformers of the protein.

Incubation of WT GST P1-1 with *cis*-DDP resulted in complete cross-linking of the dimer during the first 24 h (Fig. 3 *A*, Inset), with 2 bands, migrating at ∼49.5 and 46 kDa, appearing in the gel. With time, the lower molecular band was noticeably more intense. Multiple higher-molecular-weight bands were observed after 8 h, possibly due to the formation of oligomers of the enzyme. ESI-MS confirmed the molecular mass of the dimer species as 46,433 Da for WT GST P1-1 (Fig. 3 *A*, peak C). ESI-MS analysis after 8 h of incubation identified equivalent peaks in both the C47S and C101S mutant samples (Fig. 3 *B* and *C*, peak C). After 8 h of incubation with *cis*-DDP, the WT spectra showed an additional 3 peaks (Fig. 3 *A*, peaks E, F, and G) corresponding to the dimeric form of the WT enzyme with 2 (peaks E and F) or 3 (peak G) Pt species (Table 2). The C47S mutant spectra suggest the formation

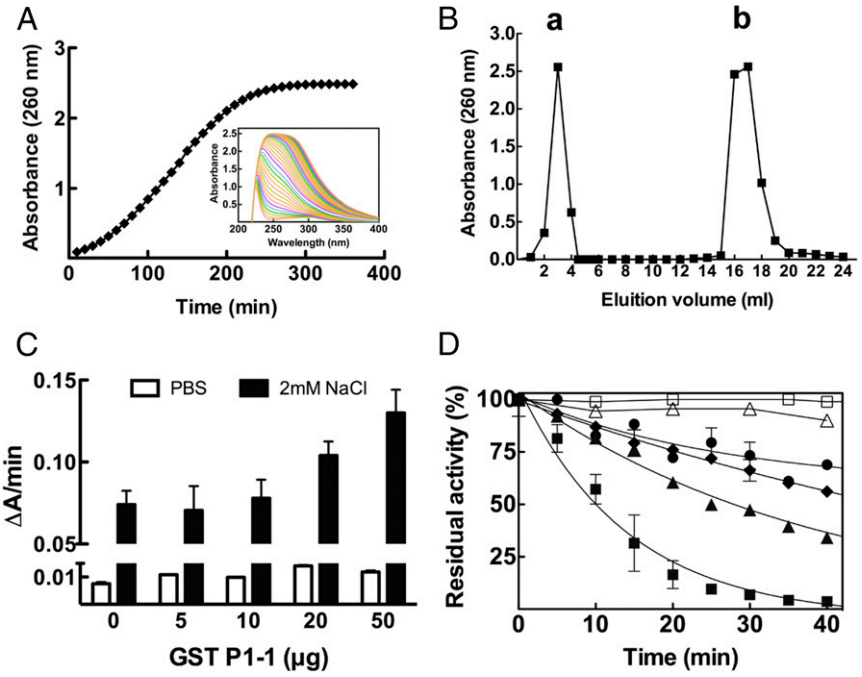

Fig. 2. *cis*-DDP–GSH adduct formation is not affected by GST P1-1 enzymatic activity. (*A*) UV spectral change during the reaction of *cis*-DDP with GSH. *cis*-DDP (1 mM) was incubated with GSH (2 mM) in PBS at 37 °C for 6 h. Every 10 min, the adduct formation was followed spectrophotometrically by measuring its absorbance at 260 nm. (*Inset*) The UV spectral change during 6 h. (*B*) Purification of the *cis*-DDP adduct of GSH. After incubation of *cis*-DDP with GSH, the reaction product was eluted from an anion-exchange column with 0.2 M HCl, and the elution profile was monitored at 260 nm. Peak a represents the unbound *cis*-DDP while peak b contains the GS-Pt adducts collected after elution with 0.2 M HCl. (*C*) Reaction of *cis*-DDP with GSH in the presence of GST P1-1. The rate of adduct formation, either in PBS or in 2 mM NaCl (pH 7.4), was followed at 260 nm at 37 °C for 10 min and reported as the change in absorbance per minute (ΔA/min), in the absence or in the presence of increasing amounts of GST P1-1. (*D*) Time course inactivation of GST P1-1 and its mutants in the presence of *cis*-DDP. □, GST P1-1 alone as control; △, GST P1-1 + 10 mM GSH + 1 mM *cis*-DDP in PBS; ●, GST P1-1 + 1 mM *cis*-DDP in PBS; ♦, Cys101Ser + 1 mM *cis*-DDP in 2 mM NaCl; ▲, Cys47Ser + 1 mM *cis*-DDP in 2 mM NaCl; ■, GST P1-1 + 1 mM *cis*-DDP in 2 mM NaCl. Data represent means ± SD of 3 independent experiments.

of multiple covalent adducts containing 2 Pt species with or without chloride ligands (Fig. 3*B*, peaks, D, E, and F). In contrast, the C101S mutant appeared to have a single dimeric species (Fig. 3 *C*, peak L), but multiple monomeric adducts attributed to C101S with 1 or 2 Pt species (Fig. 3 *C*, peaks F, G, H, and I; see also Table 2). The data of the C101S mutant are also consistent with the gel electrophoresis experiments in which a band was observed around 50 kDa before the addition of *cis*-DDP that intensified with time, but did not represent the majority of the protein. Rather, a laddering effect of higher-molecular-weight species accounts for the majority of the protein species at 72 h. The rate of intersubunit cross-linking of all of the WT, C47S, and C101S proteins was accelerated as the concentration of *cis*-DDP increased (*SI Appendix*, Fig. S2).

Structure of GST P1-1–*cis*-DDP Complex in the Absence of GSH. The crystal structure of WT GST P1-1 complexed to *cis*-DDP was determined to a resolution of 1.9 Å. *Cis*-DDP was found to bind to the dimer interface of WT GST P1-1 in 2 different modes. In the major binding mode, *cis*-DDP is bound to C101 of each subunit, causing 2 of its ligands to be displaced (Fig. 4). Alternatively, *cis*-DDP binds to the protein via just one C101 ligand, termed the minor binding mode. The occupancy for the Pt in the major mode refines to 0.7, while that in the minor mode refines to 0.6. In the major binding mode, the cysteine residues bind to the Pt ion in a *trans* arrangement, suggesting one chloride/aquo and one amine ligand have been displaced. Binding of protein thiols to *cis*-DDP can exert a strong *trans* influence that is known to lead to the displacement of Pt-bound amine ligands (35). The density maps showed no evidence of ligands other than the cysteines, possibly because they are obscured due to the strong scattering of the electron-dense Pt ion, although more ligands are required to complete the expected square planar coordination geometry of the Pt(II) ion. The Pt–sulfur bond lengths for the major *cis*-DDP binding mode are around 2.3 Å, which are within the range 2.26 to 2.80 Å, similar to values observed in crystal structures of other Pt–sulfur complexes (36, 37).

Superposition of the WT GST P1-1–*cis*-DDP complex onto the GSH complex structure (PDB ID no. 5GSS) (38) shows that the protein structures are essentially identical with an rms deviation using secondary structure matching for 389 residues of 0.3 Å. There are no significant movements of side chains in the active site or at the dimer interface, with one exception. The region around helix α2 exhibited poor electron density in the *cis*-DDP complex, consistent with the helix being highly mobile. Similar observations have been made previously for other GST P1-1 crystal structures with empty G sites (39). In subunit A, electron density for residues 36 to 45 is absent, whereas in subunit B, electron density for residues 35 to 37 and 39 to 46 is absent, although that for residues 47 to 51 is visible but of poor quality. Of particular note is the extensive water network that is normally observed at the dimer interface, including a ring of 5 water molecules that surround C101, which is severely disrupted by Pt binding.

Structure of GST P1-1–*cis*-DDP Complex in the Presence of GSH. The crystal structure of WT GST P1-1 bound to GSH and complexed to *cis*-DDP was determined to a resolution of 1.8 Å. The structure revealed 3 Pt atoms bound at the dimer interface in the major and minor binding modes described above, albeit at significantly lower occupancies than in the GSH-free structure (the level of *cis*-DDP for protein binding is presumably significantly reduced in the presence of free GSH). The satellite Pt refine to

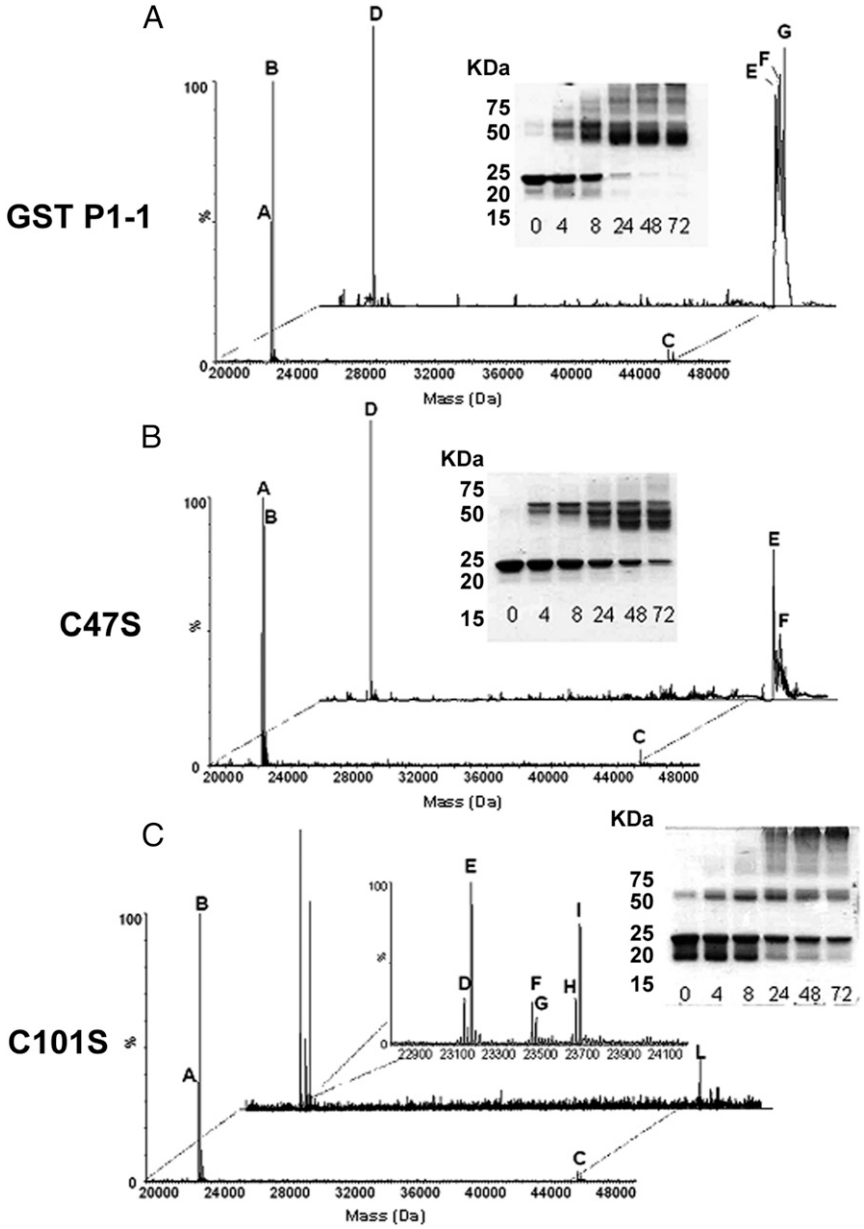

Fig. 3. *cis*-DDP acts as an effective alkylating agent of GST P1-1, in the absence of GSH, by cross-linking both subunits. (*A*–*C*) Deconvoluted ESI-MS spectra of 50 μM GST P1-1 (*A*), C47S (*B*), and C101S (*C*) after 8 h of incubation at 37 °C in the absence or presence of 50 μM *cis*-DDP. Peaks are labeled with letters, and the corresponding molecular masses are reported in Table 2. (*A*–*C*, *Insets*) The time course analysis by SDS/PAGE, under nonreducing conditions of the incubation mixture for up to 72 h.

an occupancy of 0.2, and the major Pt to 0.3. In this structure, the side chains of C101 could be built in 2 alternative conformations, with the Pt–sulfur distances consistent, with one conformation binding Pt (the same conformation observed in the GSH-free structure), and the other conformation being one that is adopted when no Pt is bound. A GSH molecule was found bound at the G site of each subunit, as observed previously for other GSH complexes, but there was no evidence of a Pt ion bound to the GSH. The occupancy of bound GSH was refined to 0.65. Comparison with the GSH-free complex described above shows that the protein structures are essentially identical for 389 residues, with an rms deviation of 0.3 Å. In this structure, however, several of the dimer-interface water molecules observed in the apo structure, but not in the GSH-free structure described above, are present. In the GSH-bound structure, helix α2 is well ordered.

Discussion

The use of the highly successful anticancer drug *cis*-DDP is limited by innate and acquired drug resistance. Although this process is multifactorial, GST P1-1 has been implicated in the resistance mechanism, and elevated GST P1-1 expression can occur in response to drug treatment but commonly occurs as part of the cancer phenotype irrespective of drug exposure. Given that, it is widely accepted that most cancer drugs are not good substrates for GST P1-1, and the role of this enzyme in drug resistance may be unrelated to GSH conjugation but involves, instead, one of the other functions of GST P1-1 (40). GST P1-1, unlike other GST proteins, has solvent-accessible cysteine residues that act as regulatory sensors. Specifically, posttranslational modifications of C47 are thought to modify the function of the protein, with *S*-glutathionylation leading to oligomerization and

Table 2. Observed mass peaks of GST P1-1 and its mutant forms incubated with *cis*-DDP

Enzyme	Peak	Molecular mass, Da	Assignment	Relative abundance, %
GST P1-1	A	23,216	GST P1-1 monomer	50
	B	23,347	GST P1-1* monomer	100
	C	46,433	GST P1-1 dimer	4
	D	23,216	GST P1-1 monomer	100
	E	46,860	GST P1-1 dimer + 2×[$Pt(NH_3)$]	74
	F	47,093	GST P1-1 dimer + 2×[$Pt(NH_3)$] + [$Pt(NH_3)_2$]	82
	G	47,429	GST P1-1* dimer + 3×[$Pt(NH_3)Cl$]	91
C47S	A	23,199	C47S monomer	98
	B	23,330	C47S* monomer	89
	C	46,398	C47S dimer	5
	D	23,753	C47S* monomer + 2×[$Pt(NH_3)$]	100
	E	46,824	C47S dimer + 2×[$Pt(NH_3)$]	54
	F	47,164	C47S dimer + 2×[$PtCl_2$] + [$Pt(NH_3)_2$]	24
C101S	A	23,199	C101S monomer	36
	B	23,330	C101S* monomer	97
	C	46,398	C101S dimer	5
	D	23,199	C101S monomer	30
	E	23,235.5	C101S monomer + MeOH	100
	F	23,524	C101S* monomer + Pt	26
	G	23,541	C101S* monomer + [$Pt(NH_3)$]	16
	H	23,734	C101S monomer + 2×[$PtCl_2$]	28
	I	23,752	C101S* monomer + 2×[$Pt(NH_3)$]	74
	L	46,464.5	C101S dimer + 2×MeOH	18

The relative abundance (%) of each peak is obtained after normalization to the tallest peak present in each spectra.
*Enzymes characterized by the presence of the N-terminal methionine residue.

carboxymethylation (41) or *S*-nitrosylation (42) reducing affinity for GSH through changes in the preequilibrium between the open and closed conformations of helix α2. Moreover, previous site-directed mutagenesis experiments have suggested that C47 is one of several key residues that cause structural perturbations of helix α2 that are, in turn, transmitted through Y49 to the neighboring subunit (43). Therefore, C47 is thought to be involved both in regulation of the transferase function of the protein and in intersubunit communication. C101 has also been implicated in regulation of activity, with reports of similar posttranslational

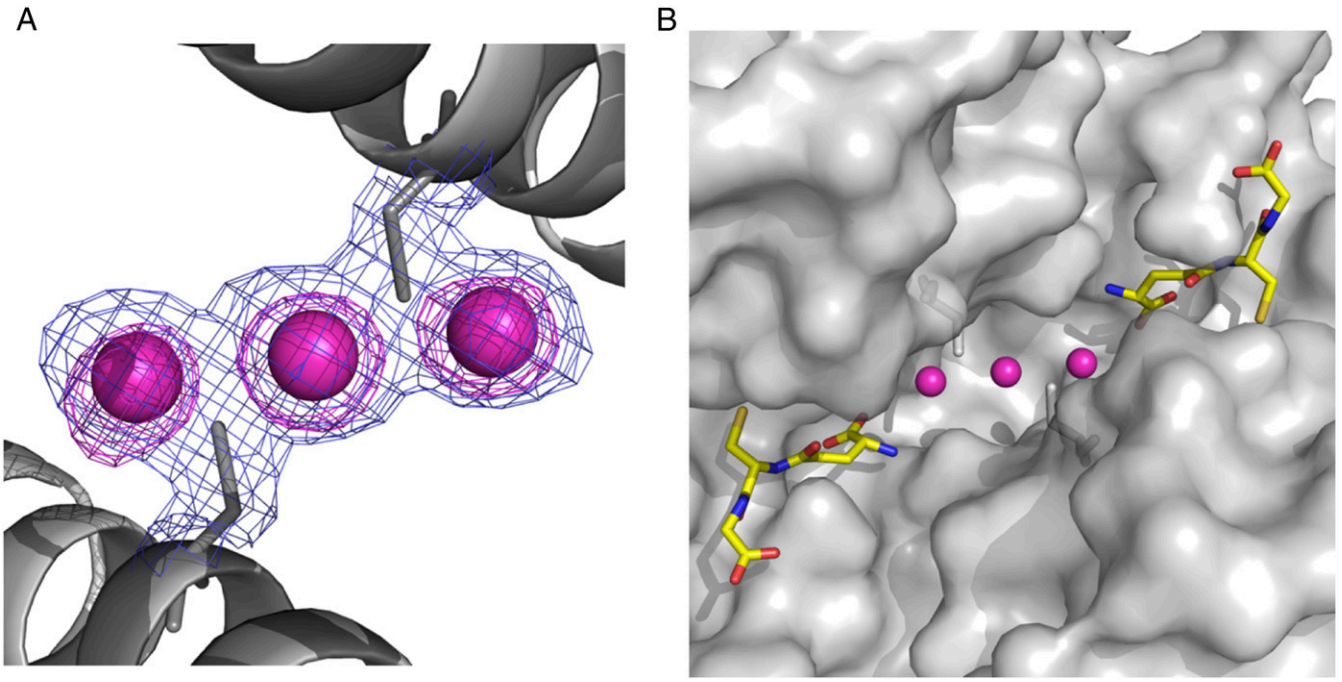

Fig. 4. *cis*-DDP can be sequestered by GST P1-1, in the presence of GSH, by binding at the dimer interface of the enzyme. (*A*) Final ($2F_o - F_c$) electron density map (contour level 1σ in blue) and anomalous difference Fourier maps (contour at 4σ in pink) focused on the dimer interface. The Pt ions are designated by the purple spheres. (*B*) Surface representation showing the Pt-binding site in relation to the active sites. The purple spheres are the Pt ions, and GSH is shown in stick fashion with carbon bonds in yellow, nitrogen atoms in dark blue, oxygen atoms in red, and sulfur atoms in gold.

modifications to those of C47, but to a lesser extent. In addition, C47–C47 intersubunit and C47–C101 intrasubunit disulfide binding can occur, which inactivates the protein for GSH transferase activity (21).

To investigate the role of C47 and C101 in the direct interaction of GST P1-1 with *cis*-DDP, plasmids coding for the WT and cysteine mutant enzymes were transfected into neuroblastoma SH-SY5Y cells. These cells were treated with *cis*-DDP and then tested for cell viability and death. Cell viability studies show that GST P1-1 overexpression confers significant protection against *cis*-DDP and reduces apoptosis induced by the drug at any dose administered, confirming the role of GST P1-1 in *cis*-DDP resistance. Of note, single point mutations of the cysteine residues affording the C47S or C101S variants reduce this protection, giving an order of *cis*-DDP sensitivity, determined by the proliferation assay and FACS analysis, as C101S > C47S > WT GST P1-1. Therefore, C101 appears to be more important because mutation of this residue makes cells more sensitive to *cis*-DDP compared with mutation of C47. C101 is more solvent accessible than C47, although, surprisingly, it has been relatively overlooked in previous studies compared with C47. Platination of C101 cannot sterically hinder GSH binding based on its location in the crystal structures. Therefore, the observation that the C101 mutant has a greater effect on *cis*-DDP resistance compared with mutation of C47 suggests that the mechanism may not involve GSH conjugation. Furthermore, the rate of in vitro formation of the *cis*-DDP adduct with GSH only slightly changes in the presence of the enzyme. Thus, the proposition that the role of GST P1-1 in *cis*-DDP inactivation is due to enzymatic conjugation of GSH with *cis*-DDP is not supported (14, 44, 45), but the GST P1-1–induced resistance to *cis*-DDP–induced cell death is instead mediated by one of its other functions (40). Note that it has also been suggested that the isoenzyme alpha 1 (GST A1-1) is also involved in *cis*-DDP resistance, but the biochemical mechanism underlying GST A1-1–mediated *cis*-DDP resistance has not been clarified (46).

The crystal structure of WT GST P1-1 in the presence of *cis*-DDP shows Pt binding in 1 of 2 different modes at the dimer interface of the protein, both involving C101 as ligands, further confirming the role of C101 in *cis*-DDP binding. GST P1-1 appears to sequester the Pt species, offering protection against cytotoxicity and cell death. The major binding mode shows *cis*-DDP mediating an intersubunit cross-link via the C101 residues, whereas the minor binding mode shows *cis*-DDP bound to a single C101 and possibly represents an intermediate stage before intersubunit cross-linking is complete. Pt sequestration does not cause substantial changes in the conformation of the protein, but notably, there is an increase in mobility of helix α2, which is most likely due to the absence of GSH from the G site and also perhaps due to Pt binding to C47. It is worth noting that the interaction of GST P1-1 with *cis*-DDP inactivates the enzyme, in the absence of GSH, in a time-dependent manner. The order of inactivation follows the order WT–Pt > C47S–Pt > C101S–Pt, which is inversely related to the order of *cis*-DDP sensitivity as measured by the proliferation assay. In contrast, incubation of GST P1-1 with *cis*-DDP in the presence of GSH preserves the transferase function. However, the crystal structure clearly shows Pt and GSH binding to different sites, and thus the preserved transferase function is not due to GSH sterically inhibiting Pt binding, indicating that in the intracellular GSH environment GST P1-1 is able to both sequester Pt and conjugate GSH to hydrophobic substrates such as CDNB (1-cloro-2,4-dinitrobenzene).

MS and gel electrophoresis studies further confirmed the role of the C101 residue in *cis*-DDP intersubunit cross-linking. Indeed, incubation of GST P1-1 and C47S with *cis*-DDP resulted in significant enzyme dimerization, apparent from the relative abundances calculated for each species of the enzyme (Table 2). In contrast, in the C101S mutant, dimerization is hardly observed, strongly confirming that Pt-induced cross-linking requires the C101 residue. Based on these data, we can also suggest that the enzyme accommodates up to 3 Pt ions per dimer, presumably at the various cysteine positions. These observations are further confirmed by the altered cytotoxicity of *cis*-DDP after treating SH-SY5Y cells transfected with the WT enzyme and its cysteine mutants. In particular, in the absence of C101, *cis*-DDP is not sequestered by the enzyme and its cytotoxicity is almost comparable to that exerted on nontransfected cells (Fig. 1*B*). The removal of both cysteines (C101S/C47S mutant) eliminates all possible *cis*-DDP anchor points on the enzyme, allowing it to exert its cytotoxic action unperturbed (Fig. 1*B*). Moreover, a Pt concentration dependence is observed in the formation of multiple Pt interactions, with a higher ratio of Pt accelerating the rate of cross-linking and progression toward a single species (*SI Appendix*, Fig. S2).

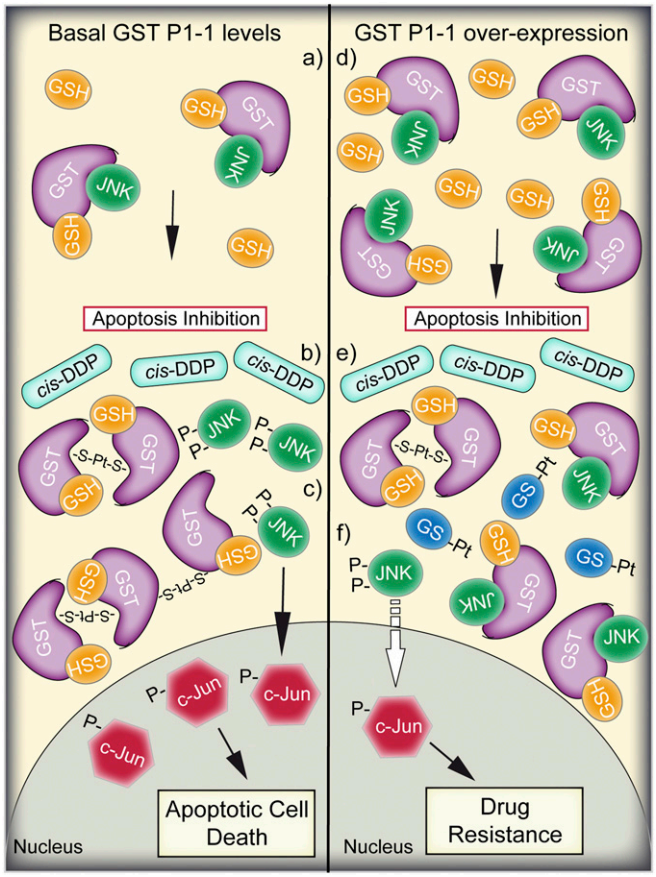

Fig. 5. Cartoon representation of the proposed mechanism of GST P1-1–mediated resistance to *cis*-DDP. (*Left*, *a*) In nonstressed cells, in the presence of basal expression levels of GST P1-1, the monomeric (or dimeric enzyme) is complexed with GSH and JNK, maintaining low JNK activity and thus inhibiting apoptotic cell death. (*Left*, *b*) Following *cis*-DDP treatment and intracellular activation, Pt ions coordinate to 2 or more subunits of GST P1-1 through the cysteine residues. (*Left*, *c*) GST P1-1 oligomerization-induced JNK release and its subsequent activation via phosphorylation leads to apoptotic cell death. (*Right*) In cells characterized by GST P1-1 overexpression and higher GSH content (i.e., cancer cells), the GST P1-1 monomers and dimers are complexed with JNK (*d*), and upon *cis*-DDP treatment (*e*), the released Pt ions are both sequestered by GST P1-1 and spontaneously conjugated to GSH (GS-Pt). However, the GST P1-1 expression levels are so high (*f*) that only a small amount of GST P1-1 dissociates from JNK, which is insufficient to activate the apoptotic signaling cascade.

The data show that *cis*-DDP is not a substrate for the GSH transferase activity of GST P1-1. Rather, the Pt species is sequestered and inactivated at the dimer interface where interactions with C101 are transmitted to the active site via helix α2. Thus, GST P1-1 is able to induce *cis*-DDP resistance in cancer cells through its function as a ligandin, while leaving its enzymatic activity intact, and possibly affecting GST P1-1 signaling function. Indeed, GST P1-1 binding to JNK prevents JNK phosphorylation, which is required for downstream apoptosis signaling (31, 32, 47–49). When GST P1-1 is cross-linked, for example via disulfide bridges, due to UV (ultraviolet) irradiation or oxidative stress, JNK is released and activated (47), signaling for apoptosis. It could be postulated that overexpression of GST P1-1, besides sequestering Pt via C101 binding and thus preventing Pt-mediated apoptosis, could also impair sufficient release of JNK to trigger the cell death. Another important aspect in the process of acquisition of *cis*-DDP resistance in cancer cells concerns the intracellular content of GSH (Fig. 5). It has been shown that GSH tends to be elevated in breast, ovarian, head and neck, and lung cancer (50), and it is known, and further demonstrated here, that intracellular GSH can conjugate with *cis*-DDP spontaneously, significantly lowering its bioavailability. Together, our results suggest that elevated GST P1-1 expression plays an important cytoprotective role against *cis*-DDP through Pt sequestration, which could confer resistance to chemotherapy, due to the intracellular transporter function of GST P1-1 rather than via the GSH transferase activity previously reported. However, considering the multiple levels of action of GST P1-1, the importance of this mechanism relative to other *cis*-DDP detoxification/resistance mechanisms remains to be established. Moreover, the relative contribution of this mechanism is expected to be highly dependent on the type of cancer or cancer cell line.

Materials and Methods

Cell Cultures. Human neuroblastoma SH-SY5Y cells were purchased from the European Collection of Cell Cultures (Salisbury, United Kingdom) and grown in Dulbecco's modified Eagle's F12 medium supplemented with 10% (vol/vol) heat-inactivated fetal bovine serum, 100 U/mL penicillin, and 100 μg/mL streptomycin, in a humidified atmosphere with 5% (vol/vol) CO_2 in air.

Cell Lysis and Protein Concentration Determination. Cells were lysed in 10 mM Tris·HCl (pH 7.4) containing 10 mM DTT and 10 mM phenylmethylsulfonyl fluoride, through 3 5-s cycles of sonication. After centrifugation for 20 min at 13,000 rpm at 4 °C, protein concentration was determined using the Bradford method (Bio-Rad).

GST P1-1 Enzymatic Activity. The enzymatic activity of WT or mutants was assayed spectrophotometrically, following the method described by Habig and Jakoby (51).

Western Blotting. Forty micrograms of total protein extracted from cell lysates was resolved on SDS/PAGE (12% gels) under nonreducing conditions and transferred on to a nitrocellulose membrane (Bio-Rad) as previously described (52). The origin of the signals related to GST P1-1 was evaluated by densitometric analysis, using actin as control.

Time Course Inactivation of GST P1-1 and Its Cysteine Mutants in the Presence of *cis*-DDP. WT GST P1-1 and its cysteine mutants (0.2 mg/mL, 10 μM in active sites) were incubated in 1 mL (final volume) of PBS or in 10 mM phosphate buffer solution plus 2 mM NaCl (pH 7.4) in the presence of 1 mM *cis*-DDP at 37 °C. At fixed times, over a period of 40 min, aliquots of sample (5 μL) were withdrawn from the mixture and assayed for residual GST activity in 100 mM phosphate buffer (pH 6.5) containing 1 mM GSH and 1 mM CDNB. As control, we incubated GST P1-1 alone or in the presence of 1 mM *cis*-DDP and 1 mM GSH, or in PBS.

ESI-MS Analysis of the GST P1-1–*cis*-DDP Interaction. WT GST P1-1 and the C47S and C101S mutants (50 μM) were each incubated with *cis*-DDP (50 μM) in potassium phosphate buffer solution (pH 7.0) at 37 °C for 8 h. The samples were diluted 1:10 in water, and 5 μL was introduced into the mass spectrometer by infusion at a flow rate of 20 μL/min with a solution of acetonitrile, H_2O, and formic acid [55:44.9:0.1, vol/vol/vol)]. A solution of phosphoric acid at 0.01% was used as an external celebrant. ESI-MS data were acquired on a Q-Tof Ultima mass spectrometer (Waters) employing a standard Z-spray ion source and operated in positive ionization mode. Instrument parameters were as follows: capillary voltage, 3.5 kV; source temperature, 80 °C; desolvation temperature, 120 °C; sample cone voltage, 50 V; desolvation gas flow, 400 L/h; acquisition window, 300 to 2,000 *m/z* in 1 s (53). Data processing was performed using the MassLynx 4.1 software.

X-Ray Crystallography. Crystallization was performed by the hanging drop vapor diffusion method as previously described (54). Crystals were grown in either the presence or absence of 10 mM GSH. Both crystal structures were solved by molecular replacement (*SI Appendix*, Table S1). The identification of Pt ions in the electron density maps was confirmed by anomalous scattering data.

Statistical Analysis. All experiments were performed at least 3 times. Statistical analysis was performed by Student's *t* test using GraphPad Prism analysis software package (Graph-Pad Software, San Diego, CA). $P < 0.05$ was considered significant.

Protein Data Bank Accession Numbers. The models have been deposited in the Research Collaboratory for Structural Bioinformatics Protein Data Bank (https://www.rcsb.org/) under PDB ID nos. 5DJM (*cis*-DDP complex) and 5DJL (*cis*-DDP–GSH complex).

ACKNOWLEDGMENTS. We would like to thank Prof. Mario Lo Bello for having dedicated his entire scientific life to the study of glutathione transferases. We thank the National Centre of Competence in Research in Chemical Biology (Switzerland) for financial support. We thank Drs. Jade Aitken, David Ascher, Mike Gorman, Guido Hansen, and Hugh Harris for advice and encouragement; and Harry Tong, other BioCARS staff, and Julian Adams for their help with data collection at the Advanced Photon Source Synchrotron. This work, including use of the BioCARS sector, was supported by the Australian Synchrotron Research Program, which was funded by the Commonwealth of Australia under the Major National Research Facilities Program. Use of the Advanced Photon Source was supported by the US Department of Energy, Basic Energy Sciences, Office of Energy Research. This work was also supported by grants from the Australian Research Council and the Australian Cancer Research Foundation (to M.W.P.), and from the Minister of Instruction, University and Research and Genesys SpA (to M.L.B.). Funding from the Victorian Government Operational Infrastructure Support Scheme to St. Vincent's Institute is acknowledged. L.J.P. was supported by a National Health and Medical Research Council of Australia (NHMRC) Dora Lush Scholarship and an International Centre for Diffraction Data Crystallography Scholarship. M.W.P. is an NHMRC Research Fellow.

1. Z. H. Siddik, Cisplatin: Mode of cytotoxic action and molecular basis of resistance. *Oncogene* **22**, 7265–7279 (2003).
2. A. Horwich, J. Shipley, R. Huddart, Testicular germ-cell cancer. *Lancet* **367**, 754–765 (2006).
3. L. Kelland, The resurgence of platinum-based cancer chemotherapy. *Nat. Rev. Cancer* **7**, 573–584 (2007).
4. R. T. Dorr, D. D. Von Hoff, Eds., "Cisplatin" in *Cancer Chemotherapy Handbook (Appleton & Lange, Norwalk, CT*, 1994), pp. 286–298.
5. G. M. Brodeur, Neuroblastoma: Biological insights into a clinical enigma. *Nat. Rev. Cancer* **3**, 203–216 (2003).
6. A. D. Kelman, H. J. Peresie, Mode of DNA binding of cis-platinum(II) antitumor drugs: A base sequence-dependent mechanism is proposed. *Cancer Treat Rep.* **63**, 1445–1452 (1979).
7. L. A. Zwelling, K. W. Kohn, Mechanism of action of cis-dichlorodiammineplatinum(II). *Cancer Treat Rep.* **63**, 1439–1444 (1979).
8. G. Chu, Cellular responses to cisplatin. The roles of DNA-binding proteins and DNA repair. *J. Biol. Chem.* **269**, 787–790 (1994).
9. E. Segal, J. B. Le Pecq, Role of ligand exchange processes in the reaction kinetics of the antitumor drug cis-diamminedichloroplatinum(II) with its targets. *Cancer Res.* **45**, 492–498 (1985).
10. M. A. Fuertes, J. Castilla, C. Alonso, J. M. Pérez, Novel concepts in the development of platinum antitumor drugs. *Curr. Med. Chem. Anticancer Agents* **2**, 539–551 (2002).
11. T. Ishikawa, F. Ali-Osman, Glutathione-associated cis-diamminedichloroplatinum(II) metabolism and ATP-dependent efflux from leukemia cells. Molecular characterization of glutathione-platinum complex and its biological significance. *J. Biol. Chem.* **268**, 20116–20125 (1993).
12. C. R. Rocha *et al.*, Glutathione depletion sensitizes cisplatin- and temozolomide-resistant glioma cells in vitro and in vivo. *Cell Death Dis.* **6**, e1727 (2015).
13. D. Lan *et al.*, Exogenous glutathione contributes to cisplatin resistance in lung cancer A549 cells. *Am. J. Transl. Res.* **10**, 1295–1309 (2018).
14. L. Sawers *et al.*, Glutathione S-transferase P1 (GSTP1) directly influences platinum drug chemosensitivity in ovarian tumour cell lines. *Br. J. Cancer* **111**, 1150–1158 (2014).

15. C. Lin, L. Xie, Y. Lu, Z. Hu, J. Chang, miR-133b reverses cisplatin resistance by targeting GSTP1 in cisplatin-resistant lung cancer cells. *Int. J. Mol. Med.* **41**, 2050–2058 (2018).
16. W. Choeyprasert *et al*., Cisplatin-induced ototoxicity in pediatric solid tumors: The role of glutathione S-transferases and megalin genetic polymorphisms. *J. Pediatr. Hematol. Oncol.* **35**, e138–e143 (2013).
17. M. H. Hanigan, P. Devarajan, Cisplatin nephrotoxicity: Molecular mechanisms. *Cancer Ther.* **1**, 47–61 (2003).
18. L. Fliedl *et al*., Controversial role of gamma-glutamyl transferase activity in cisplatin nephrotoxicity. *ALTEX* **31**, 269–278 (2014).
19. G. Chu, R. Mantin, Y. M. Shen, G. Baskett, H. Sussman, Massive cisplatin overdose by accidental substitution for carboplatin. Toxicity and management. *Cancer* **72**, 3707–3714 (1993).
20. C. R. Wolf, B. K. Park, N. Kitteringham, D. Otto, C. H. Henderson, Functional and genetic characterisation of glutatione *S*-transferase π. *Chem. Biol. Interact.* **133**, 280–284 (2001).
21. G. Ricci *et al*., Redox forms of human placenta glutathione transferase. *J. Biol. Chem.* **266**, 21409–21415 (1991).
22. M. Lo Bello *et al*., Mutations of Gly to Ala in human glutathione transferase P1-1 affect helix 2 (G-site) and induce positive cooperativity in the binding of glutathione. *J. Mol. Biol.* **284**, 1717–1725 (1998).
23. H. Y. Lim, Q. S. Ho, K. P. Wong, Interplay of metabolizing enzymes and transporter of xenobiotics. *Xenobiotica* **46**, 25–33 (2016).
24. G. Gaudiano *et al*., Lack of glutathione conjugation to adriamycin in human breast cancer MCF-7/DOX cells. Inhibition of glutathione S-transferase p1-1 by glutathione conjugates from anthracyclines. *Biochem. Pharmacol.* **60**, 1915–1923 (2000).
25. D. Rolland, M. Raharijaona, A. Barbarat, R. Houlgatte, C. Thieblemont, Inhibition of GST-pi nuclear transfer increases mantle cell lymphoma sensitivity to cisplatin, cytarabine, gemcitabine, bortezomib and doxorubicin. *Anticancer Res.* **30**, 3951–3957 (2010).
26. M. L. O'Brien, K. D. Tew, Glutathione and related enzymes in multidrug resistance. *Eur. J. Cancer* **32A**, 967–978 (1996).
27. R. Edwards, D. P. Dixon, V. Walbot, Plant glutathione S-transferases: Enzymes with multiple functions in sickness and in health. *Trends Plant Sci.* **5**, 193–198 (2000).
28. L. Prade, R. Huber, B. Bieseler, Structures of herbicides in complex with their detoxifying enzyme glutathione S-transferase–Explanations for the selectivity of the enzyme in plants. *Structure* **6**, 1445–1452 (1998).
29. I. Listowsky, M. Abramovitz, H. Homma, Y. Niitsu, Intracellular binding and transport of hormones and xenobiotics by glutathione-S-transferases. *Drug Metab. Rev.* **19**, 305–318 (1988).
30. A. J. Oakley, M. Lo Bello, M. Nuccetelli, A. P. Mazzetti, M. W. Parker, The ligandin (non-substrate) binding site of human Pi class glutathione transferase is located in the electrophile binding site (H-site). *J. Mol. Biol.* **291**, 913–926 (1999).
31. T. Wang, P. Arifoglu, Z. Ronai, K. D. Tew, Glutathione S-transferase P1-1 (GSTP1-1) inhibits c-Jun N-terminal kinase (JNK1) signaling through interaction with the C terminus. *J. Biol. Chem.* **276**, 20999–21003 (2001).
32. A. De Luca, L. Federici, M. De Canio, L. Stella, A. M. Caccuri, New insights into the mechanism of JNK1 inhibition by glutathione transferase P1-1. *Biochemistry* **51**, 7304–7312 (2012).
33. J. I. Fletcher *et al*., N-Myc regulates expression of the detoxifying enzyme glutathione transferase GSTP1, a marker of poor outcome in neuroblastoma. *Cancer Res.* **72**, 845–853 (2012).
34. M. Lo Bello *et al*., Human glutathione transferase P1-1 and nitric oxide carriers; a new role for an old enzyme. *J. Biol. Chem.* **276**, 42138–42145 (2001).
35. A. I. Ivanov *et al*., Cisplatin binding sites on human albumin. *J. Biol. Chem.* **273**, 14721–14730 (1998).
36. A. Marzotto, Effect of UO2+2 and PtCl2-4 ions on the structure and function of ribonuclease A. *Chem. Biol. Interact.* **14**, 383–391 (1976).
37. G. J. Grant, J. A. Pool, D. G. VanDerveer, Chiral effects on a fluxional ligand: Chiral diphosphine platinum(II) complexes with thiacrowns. *Dalton Trans.*, 3981–3984 (2003).
38. A. J. Oakley *et al*., The structures of human glutathione transferase P1-1 in complex with glutathione and various inhibitors at high resolution. *J. Mol. Biol.* **274**, 84–100 (1997).
39. A. J. Oakley, M. Lo Bello, G. Ricci, G. Federici, M. W. Parker, Evidence for an induced-fit mechanism operating in pi class glutathione transferases. *Biochemistry* **37**, 9912–9917 (1998).
40. C. Peklak-Scott, P. K. Smitherman, A. J. Townsend, C. S. Morrow, Role of glutathione S-transferase P1-1 in the cellular detoxification of cisplatin. *Mol. Cancer Ther.* **7**, 3247–3255 (2008).
41. C. L. Grek, J. Zhang, Y. Manevich, D. M. Townsend, K. D. Tew, Causes and consequences of cysteine S-glutathionylation. *J. Biol. Chem.* **288**, 26497–26504 (2013).
42. D. Balchin, L. Wallace, H. W. Dirr, S-nitrosation of glutathione transferase p1-1 is controlled by the conformation of a dynamic active site helix. *J. Biol. Chem.* **288**, 14973–14984 (2013).
43. G. Ricci *et al*., Structural flexibility modulates the activity of human glutathione transferase P1-1. Role of helix 2 flexibility in the catalytic mechanism. *J. Biol. Chem.* **271**, 16187–16192 (1996).
44. S. Goto *et al*., Overexpression of glutathione S-transferase pi enhances the adduct formation of cisplatin with glutathione in human cancer cells. *Free Radic. Res.* **31**, 549–558 (1999).
45. M. Pasello *et al*., Overcoming glutathione S-transferase P1-related cisplatin resistance in osteosarcoma. *Cancer Res.* **68**, 6661–6668 (2008).
46. M. Zou *et al*., Glutathione S-transferase isozyme alpha 1 is predominantly involved in the cisplatin resistance of common types of solid cancer. *Oncol. Rep.* **41**, 989–998 (2019).
47. V. Adler *et al*., Regulation of JNK signaling by GSTp. *EMBO J.* **18**, 1321–1334 (1999).
48. T. Asakura *et al*., Conformational change in the active center region of GST P1-1, due to binding of a synthetic conjugate of DXR with GSH, enhanced JNK-mediated apoptosis. *Apoptosis* **12**, 1269–1280 (2007).
49. P. Turella *et al*., Proapoptotic activity of new glutathione S-transferase inhibitors. *Cancer Res.* **65**, 3751–3761 (2005).
50. M. P. Gamcsik, M. S. Kasibhatla, S. D. Teeter, O. M. Colvin, Glutathione levels in human tumors. *Biomarkers* **17**, 671–691 (2012).
51. W. H. Habig, W. B. Jakoby, Assays for differentiation of glutathione S-transferases. *Methods Enzymol.* **77**, 398–405 (1981).
52. A. de Luca *et al*., Treatment of doxorubicin-resistant MCF7/Dx cells with nitric oxide causes histone glutathionylation and reversal of drug resistance. *Biochem. J.* **440**, 175–183 (2011).
53. F. Pelletier *et al*., Development of bimetallic titanocene-ruthenium-arene complexes as anticancer agents: Relationships between structural and biological properties. *J. Med. Chem.* **53**, 6923–6933 (2010).
54. E. Cesareo *et al*., Nitrosylation of human glutathione transferase P1-1 with dinitrosyl diglutathionyl iron complex in vitro and in vivo. *J. Biol. Chem.* **280**, 42172–42180 (2005).